Article ID: 1:006-8775(2010) 04-0409-08

EVOLUTION OF LIQUID WATER CONTENT IN A SEA FOG CONTROLLED BY A HIGH-PRESSURE PATTERN

LI Xiao-na (李晓娜)[1], HUANG Jian (黄　健)[2], SHEN Shuang-he (申双和)[1], LIU Shou-dong (刘寿东)[1], LU Wei-hua (吕卫华)[3]

(1. Institute of Applied Meteorology, University of Nanjing Information Science & Technology, Nanjing 210044 China; 2. Guangzhou Institute of Tropical and Marine Meteorology, CMA, Guangzhou 510080 China; 3. Maoming Meteorological Bureau, Maoming 525000 China)

Abstract: On March 16–17, 2008, a sea fog occurred in Dianbai in the west of Guangdong Province and was accompanied by a high-pressure synoptic system. Using comprehensive observation datasets, this study analyzes the evolution of liquid water content during this sea fog and investigates the relationships between liquid water content and the average diameters and count densities of fog droplets, air temperature, wind speed and turbulence exchanges. The main results are presented as follows. (1) The sea fog showed a quasi-periodic oscillation characteristic, i.e., it developed, disappeared and then developed again. (2) During the sea fog, the number of fog droplets changed significantly while the changes in average diameter of the fog droplets were relatively small. The development and disappearance of the sea fog correlated significantly with the fog droplet numbers. (3) The air-cooling mechanism played a significant role in sea fog formation and development. However, the influences of this mechanism were not evident during fog persistence. (4) During sea fog formation, weak turbulence exchanges were helpful for fog formation. During sea fog development and persistence, liquid water content increased when turbulence exchanges weakened, and vice versa. The changes in turbulence exchanges were closely related to the quasi-periodic oscillations observed in sea fog presence.

Key words: high-pressure pattern sea fog; liquid water content; count density of fog droplets; average diameter of fog droplets; turbulence exchanges

CLC number: X16 **Document code:** A **doi:** 10.3969/j.issn.1:006-8775.2010.04.013

1 INTRODUCTION

Sea fog is one of the phenomena of water vapor condensation at the marine atmospheric boundary layer. Reducing both horizontal and vertical visibility over the sea and coasts, sea fog severely affects all means of transportation and is one of the main causes of serious accidents. Therefore, a better understanding of sea fog is necessary for successful marine operations. Its micro-physical structure parameters, such as the size and count density of fog droplets and liquid water content, are the main indicators of sea fog density or visibility, and they also represent the macro- and micro-physical processes that occur during fog formation, development and dissipation. These processes are greatly associated with condensation nuclei, marine and meteorological conditions. Due to the convenient observation conditions over land, many observational studies of radiation fog have been implemented internationally since the 1980s[1-3]. In China, Li et al.[4, 5] conducted a series of large-scale field observations of fog over land in Nanjing, Chongqing, and Xishuangbanna, in which they measured and compared the micro-physical structure parameters of fog in different weather and geographic conditions. Deng et al.[6] implemented a comprehensive field observation of fog over the Nanling Mountains in Guangdong Province. Recently, Sun et al.[7] analyzed the spatial-temporal variations of fog occurrence frequency in recent decades. Due to the limitations of the observation environment and technology, field observations of micro-physical structures of sea fog are rare and have only been done in Qingdao and

Received date: 2009-03-18; **revised date:** 2010-09-30
Foundation item: Natural Science Foundation of China (40675013); Project of China Meteorological Administration for New Techniques (CMATG2007M23); Planing Project of Guangdong Science and Technology Department (2006B36702005)
Biography: LI Xiao-na, M.S. candidate, primarily undertaking research on atmospheric physics.
E-mail for corresponding author: hj@grmc.gov.cn

Zhoushang. These observation results focused on measuring the scales of fog droplets, number of fog droplets and liquid water content, thus providing a preliminary understanding of the micro-physical structure of sea fog in Chinese offshore waters. However, little is known of the sea fog micro-physical structure changes that occur during sea fog evolution, especially during fog formation and development.

A continuous one-month fog observation study was conducted at a scientific experiment base on marine meteorology at Bohe by Guangzhou Institute of Tropical and Marine Meteorology (Fig. 1) in March, 2008. Using droplet spectrometers, automatic weather stations, ultrasonic wind and temperature measuring devices and other observation equipment, the study continuously measured the changes of micro-physical structure parameters during sea fog, such as surface liquid water vapor, average diameter of fog droplets, count density of fog droplets, and atmospheric stability. The study primarily analyzes the variations of micro-physical structure parameters during a sea fog that arose March 16–17, and investigates the relationships between liquid water content and surface meteorological elements and turbulence exchanges. This study's results could enhance researchers' understanding of the physical processes and mechanisms of sea fog formation, development and dissipation, and provide scientific evidence for accurate operational forecasts of sea fog.

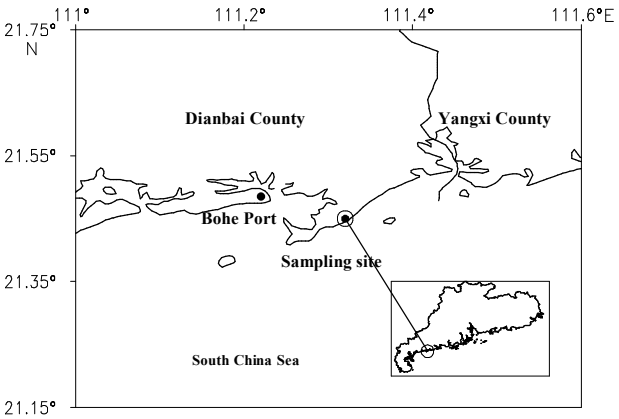

Fig. 1. The location of the observational site

2 MATERIALS AND METHODS

2.1 *Site description*

Our observation took place at the scientific experiment base on marine meteorology at Bohe, run by the Guangzhou Institute of Tropical and Marine Meteorology (Fig. 1). The experiment base is located on a coastline that stretches northeast-southwest. The Vaisala MAWS301 automatic weather station and CampbellCSAT3 ultrasonic wind/temperature devices were installed approximately at the 20-m transect from the shore of a smooth beach, where the measurements are not influenced by the terrain under the conditions of easterly and southerly winds. The droplet spectrometer was placed for field observations about 10 m from the coast and 15 m higher than sea level, in order to avoid the possible impacts of buildings and trees on fog droplet samples.

2.2 *Measurements of sea fog*

A triple-use droplet spectrometer was employed to measure the micro-physical structures of fog[4-10]. According to the principles of inertia, fog droplets are deposited on glass coated with an oil layer in the triple-use droplet spectrometer, and then the droplet size and number are manually measured[10]. The time resolution of the data obtained is often low and errors are significant. FM-100 droplet spectrometer is a type of land-based optical drop spectrometer, manufactured by Droplet Measurement Technologies Inc. (Fig. 2). Assuming that light scattered by a particle is proportional to its diameter, the FM-100 allows for the counting and characterizing of fog droplets. An emitter of a laser beam with fixed intensity and wavelength was installed in the sample area of the FM-100 droplet spectrometer. The vacuum source pulls fog particles through the sample area. Particles scatter light from the laser beam, and collecting optics guide the light into forward to masked (qualifier) detectors. The intensity of the scattered light is then related to the droplet size and to the particle concentrations[12]. The sample frequency of the FM-100 droplet spectrometer is 1 s^{-1}. The FM-100 droplet spectrometer allows for the counting and the characterization of fog droplets with diameters of 1.045, 3, 5, 7, 9, 11, 13, 15, 17, 19, 21.5, 24.5, 27.5, 30.5, 33.5, 36.5, 39.5, 43.0, 46.5, and 49 μm. The numbers of fog droplets with these 20 diameters and the sample volumes were all recorded. In this study, the data for the fog droplets were 1-min. averages.

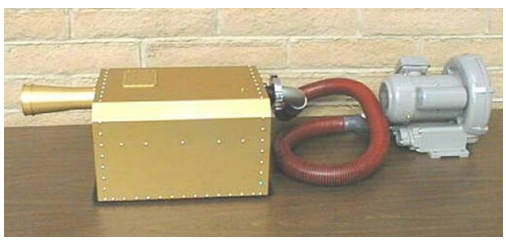

Fig. 2. DMT FM-100 droplet spectrometer

Liquid water content is computed based on the geometric mean diameter of spherical droplets and on

the corresponding number of droplets in unit volume. The relationships between liquid water content with the number and diameter of droplets and sample volume can be expressed by the following equation:

$$w = 10^{-6} \times \frac{4}{3}\pi\rho \frac{1}{V}\sum_{1}^{20} c_i \left(\frac{d_i}{2}\right)^3,$$

where w is the liquid water content (unit: g/m^3); ρ is the water density (unit: 10^6 g/m^3); V is the sample volume taken at each sampling time (unit: cm^3); c_i is the number of fog droplets with different diameters; d_i (μm) is the average diameter of corresponding sections of fog droplets diameters (i.e., if c_5=9 μ m, the corresponding c_5 means the number of fog droplets with diameters of 8–10 μm in the sample volume); and c is the count density of fog droplets. The total number of droplets in the unit sample volume can be calculated by:

$$c = \sum_{i=1}^{i=20} c_i \Big/ N$$

where N is the total number of droplets in the sample volume. The average diameter of droplets, d, is computed by:

$$d = \sum_{i=1}^{i=20} d_i c_i \Big/ N .$$

According to the similarity principle, turbulent atmospheric stability is identified by the ratio of the work done by buoyancy and that by shear stress. The atmospheric stability parameter is z/L, where z is the measurement height, and L is the Monin-Obukhov length. L is calculated by

$$L = -\frac{u_*^3 T_0}{gk(\overline{w'\theta'})}$$

where $u_* = (-\overline{u'w'})^{\frac{1}{2}}$, θ' is the measured absolute temperature, u^* is the friction velocity, k is the Kármán constant of 0.4, and g is the acceleration of gravity.

3 RESULTS

3.1 *Weather background*

A weather chart created at 20:00 (Beijing Standard Time, BST hereafter) on March 16, 2008 features a continental high over the coastal areas of China, with its center located over the Yellow Sea (Fig. 3a). The observation site was at the southwest edge of the continental high. This high contributed to a stable atmospheric stratification over the observation site while the easterly airflow of the high from the sea supplied rich warm and moist air to the observation site. A sea fog was observed under the control of this continental high, which was a typical high-pressure sea fog[13].

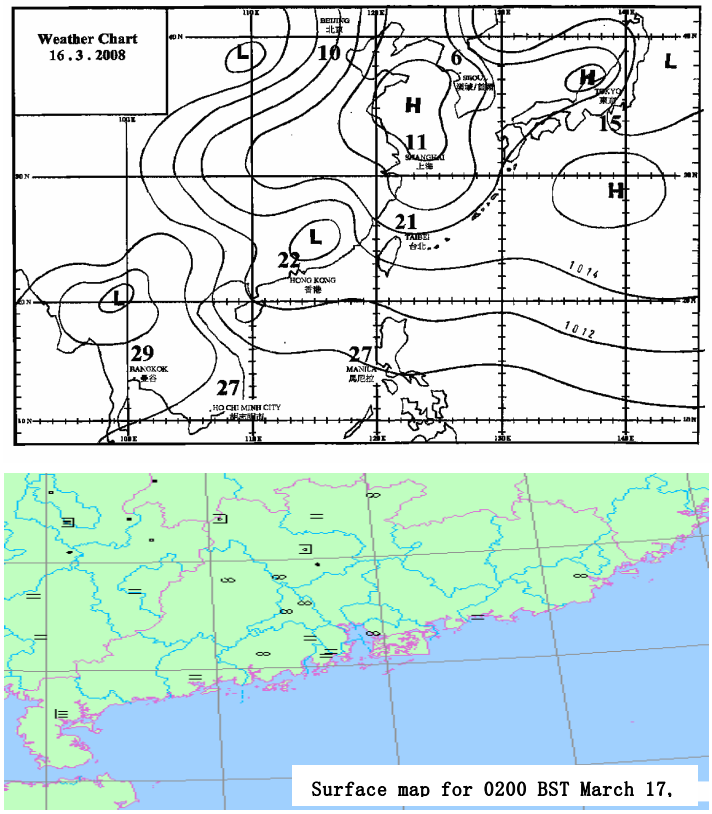

Fig. 3. (a): Surface weather map at 20:00 BST on March 16, 2008; (b): weather phenomena at the coast of Guangdong at 02:00 BST on March 17, 2008

The data available once every 3 hours from surface stations show that fog was not observed at the coastal stations at 20:00 BST on March 16th (figure omitted), and it was only observed at two stations at 23:00 BST (figure omitted). Figure 3b demonstrates that fog occurred over the coast of the western, central and eastern areas of Guangdong Province at 02:00 BST on March 17, 2008. The fog areas gradually decreased at 05:00 and 08:00 BST (figures omitted). It is found that the sea fog reached hundreds of kilometers in coverage. Figure 4 shows the changes in liquid water content and visibility over the observation site during the sea fog. Under the control of the high system, relative humidity began to increase, horizontal visibility decreased to 4–10 km, and light fog occurred on March 14, 2008 (figure omitted). At 20:30 BST March 16th, visibility sharply decreased, and fog with visibility less than 1 km first appeared. Visibility of less than 1 km persisted until early in the morning of March 17th. Visibility was the lowest at 03:00 BST on March 17th (less than 500 m) and remained at 1 km through 05:00 BST. After 07:00 BST, the fog gradually dissipated due to enhanced shortwave solar radiation. The times of fog formation and maintenance were consistent with that of the longwave atmospheric radiation cooling at night.

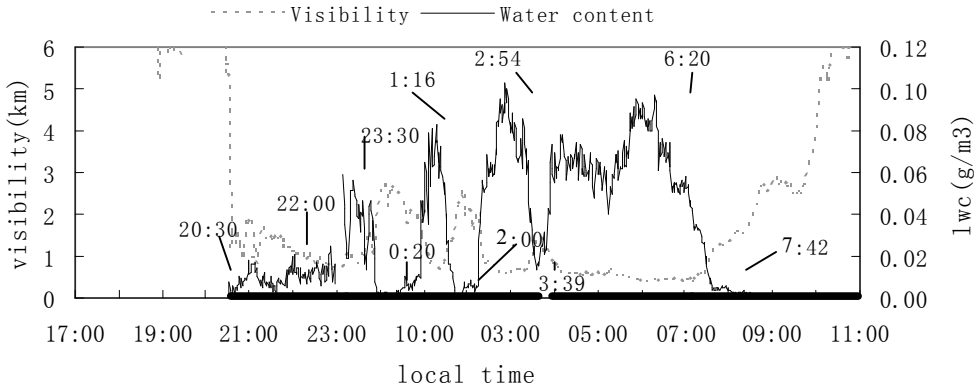

Fig. 4. Time series of liquid water content and visibility in sea fog

3.2 *Characteristics of liquid water content*

The variations in liquid water content and visibility during sea fog are shown in Fig. 4. It is noted that liquid water content is not significant during sea fog evolution, when its maximum reaches only 0.1 g/m^3. However, fog with visibility less than 1 km persisted as long as eight hours.

Figure 4 shows that during the sea fog, liquid water first occurred at 20:30 BST on March 16th. Simultaneously, visibility dropped quickly from 6 km to 1 km. Liquid water content remained between 0.01–0.02 g/m^3, and visibility stayed constant at approximately 1 km until 23:00 BST. Afterwards, liquid water content dramatically increased and showed apparent oscillatory changes and an increasing trend. Accompanying the variations in liquid water content, visibility decreased and exhibited oscillatory variations. The first oscillation with the peak value of 0.04 g/m^3 appeared at about 23:00 BST and ended at midnight. The oscillation was robust again at about 01:00 BST, and then quickly dissipated after one hour. During the third oscillation, which persisted from 02:30 to 04:00 BST, liquid water content reached its maximum of 0.1 g/m^3 at 03:00 BST, and fell back to 0.02 g/m^3 at 04:00 BST. After 04:00 BST, liquid water content increased to around 0.07 g/m^3. Although some fluctuations were observed after 04:00 BST, the magnitude of liquid water content was much less than before. Liquid water content significantly decreased because shortwave solar radiation gradually increased at 0:700 BST. At 11:00 BST, liquid water totally disappeared and visibility was about 6 km. The variations in liquid water content between 23:00 and 04:00 BST indicate that there were three significant processes of liquid water content growth and decline, and the peaks and troughs of the three oscillations were increased. In addition, the decreasing durations of liquid water content were different among the three oscillations, being approximately one hour, thirty minutes, and twenty minutes, respectively. The period of liquid water content lasted about 20–60 minutes and decreased with time, suggesting that liquid water content shows evident quasi-periodic fluctuations.

Because of the limitation of these observations, little is known about the oscillations that occurred during sea fog. In the past, researchers have generally believed that because of certain balanced states of heat and water vapor in fog, liquid water remains in a stable condition. However, our observed results of liquid water content show that the variations of sea fog are

not monotonous, but exhibit a clear development-dissipation-development process, which is particularly featured in the period between 23:00 BST on March 16, 2008 and 04:00 BST on March 17, 2008, when liquid water content increased greatly. Our observed results are in agreement with those of radiation fog[14]. For the sake of convenience, sea fog evolution is divided into four stages in terms of the characteristics of liquid water content: the formation stage (20:30–23:00 BST on March 16th), development stage (23:00 BST on March 16th to 04:00 on March 17th), persistence stage (04:00–07:00 on March 17th), and dissipation stage (after 07:30 on March 17, 2008).

3.3 *Characteristics of count density and average diameter of fog droplets*

The microphysical structure parameters used in this study were continuously measured by advanced and precise equipment, which provides high resolution fog droplets sizes, with the smallest observed diameter being 1.045 μm. Figure 5 shows the variations in liquid water content, count density and average diameter of fog droplets, as observed on March 16–17, 2008. Before sea fog formation, the count density of the droplets was 5/cm^3, and the average diameter of the droplets was about 2 μm near the surface, which can be explained by salt nuclei in the atmosphere near the sea surface[13].

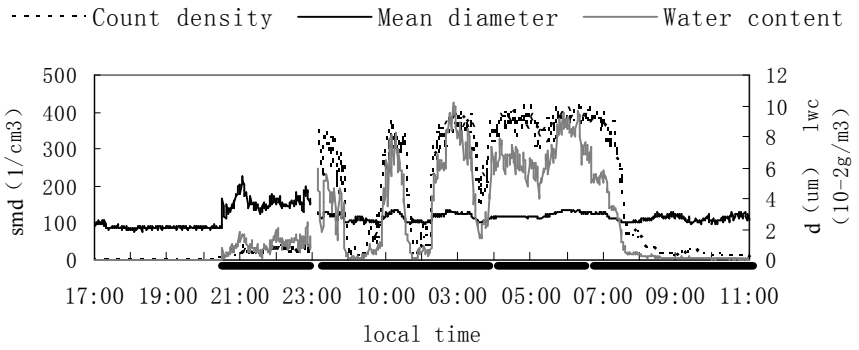

Fig. 5. Time series of liquid water content, averaged diameter and count density of droplets in sea fog

During the stage of sea fog formation, the count density of droplets—larger than before—was 50/cm^3, and the average diameter of the droplets was developing to 3–5.5 μm, which was the largest figure observed in the sea fog. The increases in count density and average diameter of droplets indicate that during fog formation, water vapor condensed on the condensation nuclei (such as the burning nuclei) which were smaller in diameter than salt nuclei, and this resulted in the increase of droplet number.

Accompanied by notable fluctuations in liquid water content, the count density of fog droplets changed significantly during sea fog development stage. The variations in the count density of fog droplets were similar to those of liquid water content. The average diameter of fog droplets fluctuated to a certain degree, while the change magnitude was small (about 2–3 μm). Although the count density of fog droplets fluctuated as well as liquid water content, the magnitude of the droplets' count density during the sea fog persistence stage was much smaller than that observed during the sea fog development stage, while the average diameter of sea fog droplets remained unchanged.

During the sea fog dissipation stage, both liquid water content and count density of fog droplets decreased quickly, and the average diameter of sea fog droplets remained constant at approximately 3 μm. This may have been the result of the temperature increase and fog droplet evaporation because of shortwave solar radiation. The evaporation of sea fog droplets led to higher relative humidity, and the larger liquid droplets were caused by the moisture absorption of salt nuclei.

Except during sea fog formation, the changes in average diameter of fog droplets were between 2–3.2 μm, and the count density of fog droplets fluctuated between 5–420 per cm^3, which was consistent with the changes in liquid water content. According to the relationships between liquid water content, count density and average diameter of fog droplets, the count density of fog droplets plays a more important role in variations of water liquid content. The large increase in liquid water droplets—particularly the small liquid water droplets—is the main reason behind sea fog development. Previous studies revealed that count density of fog droplets observed in Qingdao, Zhoushan, and Bohe of Guangdong Province were 30, 30, and 56.3 per cm^3, respectively, and the average diameters

of fog droplets were 4.5, 22.1, and 5.2 μm, respectively[15, 16]. Unlike these previously obtained results, however, this study found that the average diameter of sea fog droplets remained constant at approximately 3 μm, which was larger than the observed average diameter of salt nuclei, and the maximum count density of fog droplets was as high as 420/cm^3. These differences may be attributable to improvements of observation capabilities and measurement equipment. Due to the utilization of advanced observation equipment, the observation capacity and accuracy of small fog droplets have been significantly improved, resulting in direct decreases in the average diameter of fog droplets.

3.4 *Relationship between liquid water content and meteorological elements*

Through air-cooling or humidification, water vapor condenses and thus creates sea fog. The contact cooling, advection cooling, radiation cooling and vertical turbulence exchanges are the four primary ways to cool air[13]. Figure 6 shows the time series of liquid water content, air temperature, wind speed and direction during sea fog.

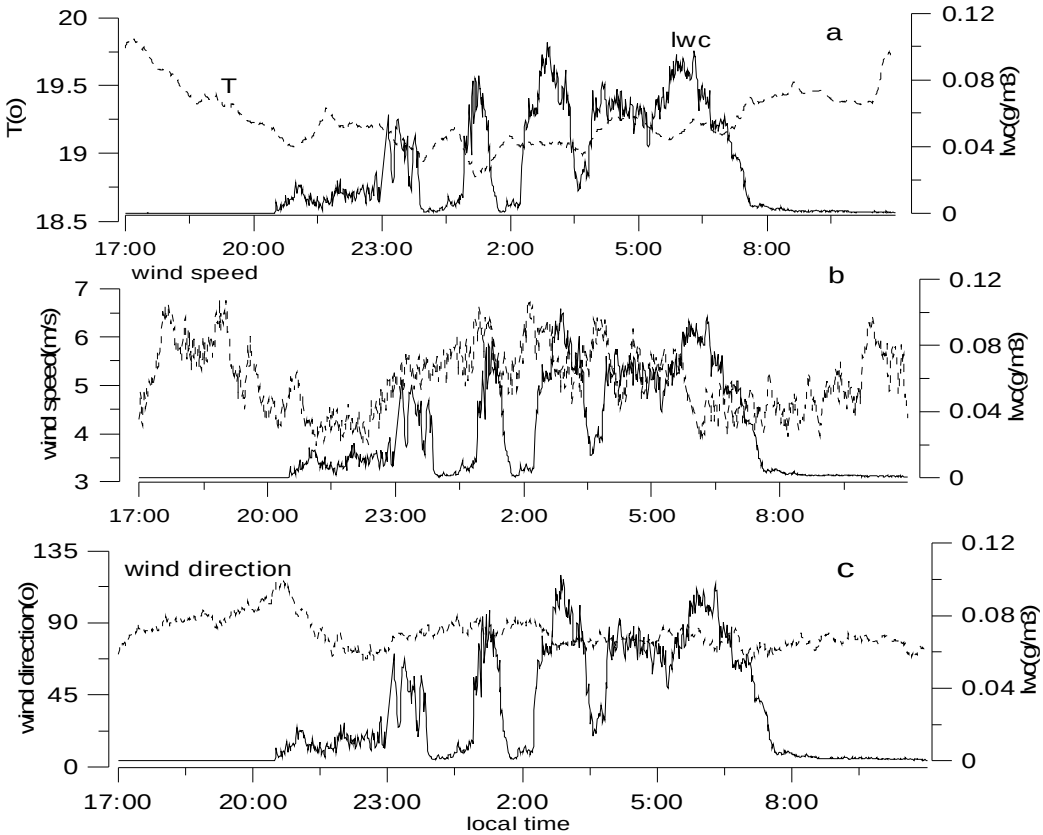

Fig. 6. Time series of liquid water content (solid line) vs. (a) air temperature, (b) wind speed and (c) wind direction

Air temperature gradually decreased after 17:00 BST on March 16th, and reached about 19°C at 20:30 BST when liquid water was first observed (Fig. 6a). During the stage of sea fog development, air temperature tended to decrease. The peaks (valleys) of liquid water content at the first and second oscillations occurred when air temperature decreased (increased), indicating that air temperature was related negatively to liquid water content. However, the inverse relationship was not evident after the third peak of liquid water content, especially during the stage of sea fog persistence. Liquid water content even increased with increases in air temperature at 04:00 and 05:00 BST. The changes in the relationship between air temperature and liquid water content suggest that the water vapor saturation and condensation are mainly the result of air-cooling effect that occurs during sea fog formation and development, while other physical mechanisms—such as warm air at the fog-top being entrained into the fog layer) in addition to air-cooling—play vital roles during sea fog persistence.

Wind speed is usually weak during radiation fog over land and generally ranges between 0–2 m/s. Wind conditions during sea fog are greatly different from those observed during radiation fog over land (Fig. 6b). Wind speed was 4–6.5 m/s during sea fog, which is higher than that the speed observed during radiation fog over land. Furthermore, wind speed varied

significantly during different sea fog stages. More specifically, wind speed tended to decrease during sea fog formation and dissipation, while it was higher during sea fog development and persistence. Wind direction was at about 70–90 degrees and changed insignificantly during sea fog (Fig. 6c). The sea fog originated from the sea and was not particularly influenced by the longwave radiation cooling from land. It is suggested that sea fog is influenced by the cooling mechanisms of air-sea interaction, longwave radiation transport between the fog layer and sea surface, and longwave radiation transport between the fog-top layer and outer space[13].

4 DISCUSSION

Recent observational and simulation studies of sea fog reveal that longwave radiation cooling at the fog-top layer and associated vertical turbulence exchanges are the main physical processes that govern sea fog formation, development and dissipation[17-19]. Atmospheric stability can be used to measure turbulence exchanges near the sea surface. If $z/L>0$, the atmosphere is stable and vertical exchanges are weakened, while if $z/L<0$, the atmosphere is unstable and vertical exchanges are strengthened. Figure 7 shows the relationship between atmospheric stability and liquid water content in the presence of sea fog, which reveals the roles of vertical turbulence exchanges in different sea fog stages. During sea fog formation, z/L ranged between -1 and 0, indicating that the atmosphere was neutral or mildly unstable near the surface and sea fog arosed with weak turbulence exchanges (Fig. 7).

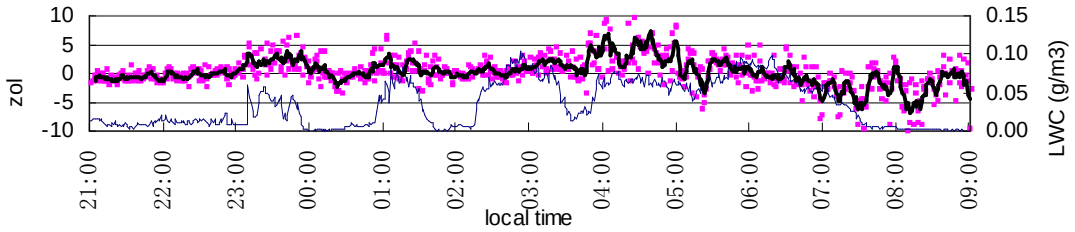

Fig. 7. Time series of liquid water content and atmospheric stability. The scatter plot denotes the atmospheric stability of 1-min. average; The thick solid line denotes the moving average line for atmospheric stability; and the fine solid line denotes liquid water content.

Liquid water content fluctuated greatly during sea fog development. When the values of z/L were positive, the peaks of liquid water content were observed, while the valley of liquid water content was observed when z/L was reduced or negative. Therefore, a stable atmosphere—i.e., reductions in or the elimination of turbulence exchanges—is helpful for sea fog development, while an unstable or neutral atmosphere—i.e., strengthened turbulence exchanges—hinders fog development and even leads to fog dissipation. The relationship between z/L and liquid water content during sea fog persistence was similar to that which occurred during sea fog development. When the atmosphere was stable, liquid water content was large, whereas it decreased quickly when z/L decreased or was negative.

During sea fog dissipation, z/L was always negative. The warming at the surface due to shortwave solar radiation enhanced vertical turbulence exchanges at the fog layer. These stronger vertical turbulence exchanges resulted in the rising of the fog-top layer and lifted the condensation level. Finally, fog was able to be elevated to form low clouds[20]. On the other hand, as fog was warmed, water vapor saturation reduced, and fog droplets evaporated, which led to the rapid decrease of liquid water content and thus fog dissipation.

There are two contradictory arguments about the relationship between fog and turbulence exchanges. One suggests that reduced or ceased turbulence exchanges is helpful for fog development. However, the other holds that fog development correlates significantly with the enhancement of turbulence exchanges. Based on the observations of radiation fog, Roach et al.[1, 2] argued that when wind speed is reduced to its minimum and turbulence exchanges activity is near zero, fog can occur. Taylor[21] and Rodhe[22] pointed out that the reduced or ceased turbulence exchanges are not necessary conditions for fog development and emphasized instead, the roles of strong vertical turbulence exchanges resulting in the saturation of air at different temperature in fog development.

In our observation, the relationship between liquid water content and atmosphere stability shows that the role of vertical turbulence exchanges differs across the distinct fog stages. During fog formation, weak vertical turbulence exchanges were helpful for fog formation, whereas during the stages of fog development and persistence when there has been some liquid water, the

enhancement of vertical turbulence exchanges could result in a decrease of liquid water content and in fog dissipation. In contrast, reduced or ceased vertical turbulence exchanges could cause increase in liquid water content and fog development. Apparently, the turbulence exchanges are closely associated with the quasi-periodic oscillations of sea fog development, dissipation and development.

5 CONCLUSIONS

(1) During sea fog evolution, liquid water content shows the quasi-periodic variations, indicating a clear development-dissipation-development evolution of sea fog.

(2)The changes in average diameter of sea fog droplets were not significant during sea fog evolution, as they were less 1 μm, especially during fog development and persistence stages. However, the count density of fog droplets varied significantly, and these variations were consistent with liquid water content variations. The count density of fog droplets plays a more significant role in water liquid content.

(3) Air temperature decreased during sea fog formation and development, indicating that the air-cooling effect was the most important physical mechanism of sea fog. However, the influences of air-cooling effect were not significant during fog persistence.

(4) Wind speed weakened during sea fog formation and dissipation, while wind speed was stronger during sea fog development and persistence. Wind direction changed insignificantly during sea fog.

(5) The weak turbulence exchanges were helpful for sea fog formation, while the enhanced (reduced) turbulence exchanges during sea fog development and persistence could result in liquid water reducing (increasing) and fog disappearing (developing). The turbulence exchanges were closely related to the quasi-periodic oscillations of sea fog.

REFERENCES:

[1] ROACH W T. On the effect of radiative exchange on the growth by condensation of a cloud or fog droplet [J]. Quart. J. Roy. Meteor. Soc., 1976, 102: 361-372.
[2] ROACH W T, BROWN R, CAUGHEY S J, et al. The physics of radiation fog Part I: A field study [J]. Quart. J. Roy. Meteor. Soc., 1976, 102: 313-333.
[3] GERBER H E. Microstructure of a radiation fog [J]. J. Atmos. Sci., 1981, 38(2):454-458.
[4] LI Zi-hua, HUANG Jian-ping. Physical structure of the five-day sustained fog around Nanjing in 1996 [J]. Acta Meteor. Sinica, 1999, 57(5): 622-631.
[5] LI Zhi-hua, ZHANG Li-min, LOU Xiao-feng. The macro-and micro-structure of winter fog in the Chongqing urban district and the physical cause of its formation [J]. J. Nanjing Inst. Meteor., 1993, 16(1): 48-54.
[6] DENG Xue-jiao, WU Dui, YE Yan-xiang. Physical characteristics of dense fog at Nanling mountain region [J]. J. Trop. Meteor., 2002, 18(3): 227-236.
[7] SUN Dan, ZHU Bin, DU Wu-peng. The temporal and spatial distribution of thick fog frequency in China [J]. J. Trop. Meteor., 2008, 24(5): 497-501.
[8] YANG Lian-su. A preliminary observations of the microphysical structure of fog in Qingdao area [J]. Marine Sci., 1985, 9(4): 49-50.
[9] XU Jing-qi, ZHANG Zheng, WEI Hao. Measurement and analysis of droplet spectrum and liquid water content of sea fog [J]. Trans. Oceanol. Limnol., 1994, 16(2):174-178.
[10] YANG Zhong-qiu, XU Shao-zhu, GEN Biao. The formation and microphysical structure of sea fog at Zhoushan in spring [J]. Acta Oceanol. Sinica, 1989, 11(4):431-438.
[11] ZHAO Bo-lin, ZHANG Ai-shen. The principle of atmospheric detection [M]. Beijing: Meteorolgical Press, 1990: 578.
[12] DMT Inc. Fog Monitor Operator Manual Doc-:0088 Revision A [Z]. 2005.
[13] WANG Bin-hua. Sea Fog [M]. Beijing: Ocean Press, 1983: 352.
[14] LALA G G, JIUSTO J E, MEYER M B, et al. Mechanisms of radiation fog formation on four consecutive nights [C]// Preprints Conf. Cloud Physics, Chicago: Amer. Meteor. Soc., 1982: 9-11.
[15] QU Feng-qiu, LIU Shou-dong, YI Yan-ming et al. The observation and analysis of sea fog event at the South China [J]. J. Trop. Meteor., 2008, 24(5): 490-496.
[16] HUANG Hui-jun, HUANG Jian, LIU Chun-xia, et al. Prediction of sea fog Guangdong coastland using the variable factors output by GRAPES model [J]. J. Trop. Meteor., 2010, 26(1): 31-39.
[17] FINDLATER J, ROACH W T, MCHUGH B C. Project Haar Air Clues [J]. The Magazine of Royal Air Force, 1985, 39(9): 350-353.
[18] LEIPPER D F. Fog on the United States West Coast: A review [J]. Bull. Amer. Meteor. Soc., 1994, 75(2): 229-240.
[19] LEWIS J M, KORACIN D, REDMOND K T. Sea fog research in the United Kingdom and United States: A historical essay including outlook [J]. Bull. Amer. Meteor. Soc., 2004, 85(3): 395-408.
[20] ROGERS D P, KORACIN D. Radiative transfer and turbulence exchanges in the cloud-topped marine atmospheric boundary layer [J]. J. Atmos. Sci., 1992, 49(16): 1 473-1 486.
[21] TAYLOR G. The formation of fog and mist [J]. Quart. J. Roy. Meteor. Soc., 1917, 43: 241-268.
[22] RODHE B. The effect of turbulence exchanges on fog formation [J]. Tellus, 1962, 14: 49-86.

Citation: LI Xiao-na, HUANG Jian, SHEN Shuang-he et al. Evolution of liquid water content in a sea fog controlled by a high-pressure pattern. *J. Trop. Meteor.*, 2010, 16(4): 409-416.